JURNAL KARTIKA KIMIA

J. Kartika Kimia, November 2025, 8, (2), 272-283
Journal homepage: http://jkk.unjani.ac.id/index.php/jkk
P-ISSN: 2655-1322 E-ISSN: 2655-0938

Experimental Synthesis and In Vivo Assessment of the Antidiabetic Activity of an Iron(III)-Glycine Complex

Pinkan Valencia[1], Yuli Ambarwati[2,*], Nurhasanah[2], Sonny Widiarto[2], Andi Setiawan[2], Kamisah Delilawati Pandiangan[2]
[1]Postgraduate Student Department of Chemistry, Lampung University, Bandar Lampung, Indonesia
[2]Department of Chemistry, Lampung University, Bandar Lampung, Indonesia
*E-mail: yuli.ambarwati@fmipa.unila.ac.id

DOI: https://doi.org/10.26874/jkk.v8i2.953

Received: 9 July 2025, *Revised*: 6 April 2026, *Accepted*: 13 April 2026, O*nline*: 26 April 2026

Abstract

Indonesia is one of the countries with a growing number of diabetes mellitus cases each year. This disease can cause damage to vital organs such as the liver, pancreas, kidneys, and heart. Type 1 diabetes is generally treated with insulin, while type 2 diabetes is commonly managed with oral medications. Recently, metal complexes have emerged as promising alternatives for antidiabetic therapy. Among these, iron(III) complexes are of interest, although research on Fe(III) complexes remains limited. This study aims to synthesize and evaluate the in vivo antidiabetic activity of an iron(III)-glycine complex. The synthesized complex appeared as an orange-brown solid with a yield of 95.02% and a sample mass of 0.267 g. UV-Vis spectrophotometric analysis showed absorption peaks at 210, 224, and 305 nm, indicating the presence of the Fe(III)-glycine complex. FTIR analysis revealed characteristic absorption bands corresponding to Fe–O at 523 cm^{-1} and Fe–N at 823 cm^{-1}. In vivo tests were conducted on mice induced with alloxan. Body weight of the mice decreased after induction but stabilized after treatment during the third and fourth weeks. The highest reduction in blood glucose levels was observed at a dose of 200 µg/kg body weight, with a 68% decrease. These results suggest that the Fe(III)-glycine complex exhibits potential as an antidiabetic agent.

Keywords: antidiabetic activity, blood glucose, iron(III)-glycine complex, metal complex

1 Introduction

Diabetes mellitus is a chronic metabolic disorder that continues to rise in prevalence worldwide. According to the 10th edition of the International Diabetes Federation (IDF) Diabetes Atlas published in 2021, approximately 537 million adults globally are living with diabetes mellitus [1]. Indonesia ranks seventh among the top ten countries with the highest number of diabetes cases, with a prevalence rate of 10.7% [2]. Diabetes mellitus comprises several types with distinct characteristics. Type 1 diabetes mellitus (T1DM) occurs due to damage to pancreatic β-cells responsible for insulin production. In the absence of sufficient insulin, blood glucose levels rise, leading to potential damage to blood vessels and vital organs such as the heart and kidneys. In contrast, type 2 diabetes mellitus (T2DM) is characterized by insulin resistance, which impairs glucose uptake and results in persistent hyperglycemia [2].

T2DM has become a major global health concern, largely driven by unhealthy lifestyle factors such as high consumption of fatty and sugary foods, physical inactivity, smoking, and excessive caloric intake [3]. The increasing prevalence of T2DM has encouraged the development of alternative therapeutic strategies, including the use of metal-based compounds. Metal therapy involves the application of transition metal ions as pharmacologically active agents [4]. Various inorganic metal complexes such as those of chromium, manganese, molybdenum, copper, cobalt, zinc, and vanadium have demonstrated promising antidiabetic properties.

Previous studies have reported significant glucose-lowering effects of several metal–amino acid complexes. For instance, Ambarwati et al. (2021) successfully synthesized a Cr(III)-glycine complex that reduced blood glucose levels by 44.12% at a dose of 200 µg/kg body weight in

diabetic rats [5]. Similarly, a Cu(II)-glycine complex showed a reduction of 41.33% under comparable conditions [6]. Additional computational and in vivo studies further support the antidiabetic potential of chromium(III) and copper(II) complexes [7–9].

Despite these advances, the use of certain transition metals such as chromium and vanadium may raise concerns related to long-term toxicity and bioaccumulation. In this context, iron particularly in the Fe(III) oxidation state offers several advantages. Iron is an essential and biologically abundant metal with relatively low toxicity at controlled levels, and it plays a critical role in numerous physiological processes. Fe(III) functions as a cofactor in various enzymatic systems, including antioxidant enzymes such as superoxide dismutase (SOD), which help mitigate oxidative stress and reduce the risk of vascular complications associated with diabetes [10]. These properties make Fe(III) a more biocompatible and potentially safer alternative compared to other transition metals.

Furthermore, amino acids such as glycine are attractive ligands due to their ability to form stable coordination complexes and their inherent biological compatibility [12]. The combination of Fe(III) with glycine is therefore expected to yield a complex with enhanced stability, bioavailability, and therapeutic potential.

Based on this rationale, the present study aims to synthesize a Fe(III)-glycine complex, characterize it using UV–Visible and FTIR spectroscopy, and evaluate its antidiabetic activity through in vivo testing in experimental animals. The findings of this study are expected to contribute to the development of safer and more effective antidiabetic therapies based on transition metal complexes.

2 Method

1.1 Materials

Ferric chloride hexahydrate ($FeCl_3 \cdot 6H_2O$), glycine, sodium hydroxide (NaOH), sodium chloride (NaCl, 0.9%), alloxan monohydrate, glibenclamide (5 mg), On Call Plus glucose test strips, male mice (Mus musculus L.), standard pellet feed, drinking water, and distilled water were used in this study. All reagents were of analytical grade and used without further purification.

1.2 Procedures

The synthesis procedure was adapted from Konapalli et al. [13] and Ambarwati et al. [6]. The Fe(III)-glycine complex was prepared using a 1:3 molar ratio of metal to ligand. Ferric chloride hexahydrate (0.27 g, 1 mmol) was dissolved in 25 mL of distilled water, and glycine (0.23 g, 3 mmol) was dissolved separately in 25 mL of distilled water. The two solutions were mixed under continuous stirring until homogeneous.

To determine the optimal synthesis conditions, the reaction mixture was refluxed at 60°C for different durations (1–5 hours) at pH 5. The yield and spectral characteristics (UV–Vis absorbance intensity and peak consistency) of the resulting complexes were evaluated to determine the optimal reaction time. Subsequently, the synthesis was repeated at different pH values (5, 6, and 7) using the previously optimized reaction time. The optimal conditions were selected based on maximum yield and consistent spectral features, and are presented in the Results section (**Fig. 1**).

Under optimal conditions (2 hours, pH 7), the reaction mixture was further processed and the resulting complex was isolated by freeze-drying for 48 hours. The dried product was weighed until a constant mass was obtained.

The synthesized complex was characterized using: UV–Visible spectroscopy (Cary UV 1010M217) in the range of 200–800 nm. FTIR spectroscopy (Cary 630) in the range of 4000–400 cm^{-1}. In addition, elemental (CHN) analysis was performed to confirm the composition and stoichiometry of the complex. The experimental percentages of carbon (C), hydrogen (H), and nitrogen (N) were compared with theoretical values calculated for the proposed $[Fe(Gly)_3]$ structure to validate the 1:3 metal-to-ligand ratio.

Male mice (Mus musculus L.) were randomly divided into experimental groups following the protocol of Ambarwati et al. [7]. The groups consisted of: (1) normal control; (2) diabetic control (negative control); (3) positive control (glibenclamide-treated); (4) $FeCl_3$-treated group; (5) glycine-treated group; and (6) Fe(III)-glycine complex-treated groups (50, 100, and 200 μg/kg body weight).

Diabetes was induced using alloxan monohydrate. It is important to note that alloxan selectively destroys pancreatic β-cells, thereby

inducing a Type 1 diabetes (insulin-deficient) model. Therefore, this study primarily evaluates the potential of the Fe(III)-glycine complex in improving hyperglycemia under insulin-deficient conditions, which may also provide insight into oxidative stress-related pathways relevant to diabetes. Blood glucose levels were monitored glucose test strips at designated time intervals.

Data were analyzed using one-way Analysis of Variance (ANOVA) to determine statistically significant differences among experimental groups. Results are expressed as mean ± standard deviation (SD), and differences were considered significant at $p < 0.05$.

To evaluate potential diabetic complications and treatment effects, vital organs (liver, kidneys, pancreas, and heart) were collected post-mortem. Histopathological and/or gross examinations were performed to assess tissue damage associated with hyperglycemia and treatment.

The drug-likeness and pharmacokinetic properties of the synthesized complex were evaluated using: (a) Lipinski's Rule of Five via the SCFBio portal; (b) ADME profiling using SwissADME; and (c) Toxicity prediction using the ProTox-II webserver.

3 Result and Discussion

Synthesis of Fe(III)-glycine Complex Compounds. The Fe(III)-glycine complex was successfully synthesized under optimal conditions at a reaction time of 2 hours and pH 7 (**Fig. 1**). The product obtained was a brownish-orange solid weighing 0.267 grams, with a yield of 95.02%. The color of the resulting complex is closely related to the chemical properties of the Fe^{3+} transition metal ion and the coordination structure of the complex. Fe^{3+} ions are known as chromophores, meaning they can absorb light in the visible region of the electromagnetic spectrum due to their partially filled d-orbitals. Electrons in these orbitals can undergo excitation, transitioning to higher energy levels. These d–d electronic transitions result in the absorption of light, particularly in the red to brown region of the spectrum, which accounts for the observed brownish-orange color of the complex [14].

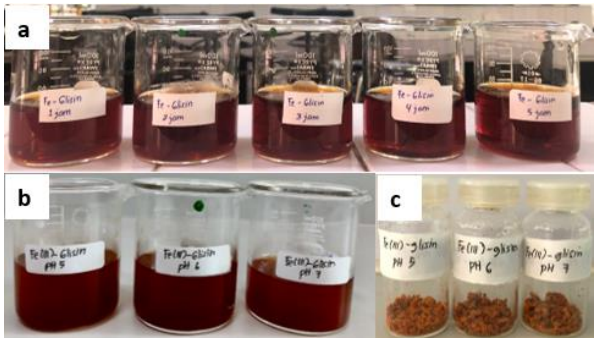

Figure 1. Fe(III)-glycine synthesis (a) time variation; (b) pH variation; (c) freeze dry results

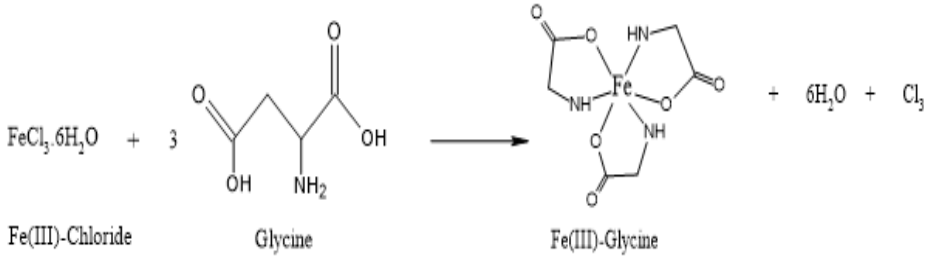

(Equation 1)

The reaction between $FeCl_3$ and glycine to form a complex compound $[Fe(Gly)_3]$ is shown in **Eq. 1**. The formation mechanism of the $[Fe(Gly)_3]$ complex begins with the substitution of chloride ions (Cl^-) in $FeCl_3 \cdot 6H_2O$ by donor groups from glycine, specifically the amino ($–NH_2$) and carboxylate ($–COO^-$) groups. This substitution occurs due to differences in ligand strength, where $–NH_2$ and $–COO^-$ are stronger electron-donating ligands compared to chloride, which is considered a weak ligand and a good leaving group (**Fig. 2**).

The $–NH_2$ and $–COO^-$ groups of glycine act as nucleophiles—chemical species that possess lone pairs of electrons and are attracted to electron-deficient centers such as the positively charged Fe^{3+} ion. This interaction leads to the

formation of coordination bonds between glycine ligands and the Fe^{3+} ion, resulting in a stable [$Fe(Gly)_3$] complex with an octahedral geometry [15].

Characterization Results of Fe(III)-glycine Complex Compounds. UV-Vis spectrophotometric characterization was performed to determine the maximum wavelength (λmax) absorption of the [$Fe(Gly)_3$] complex, as shown in **Fig. 3**.

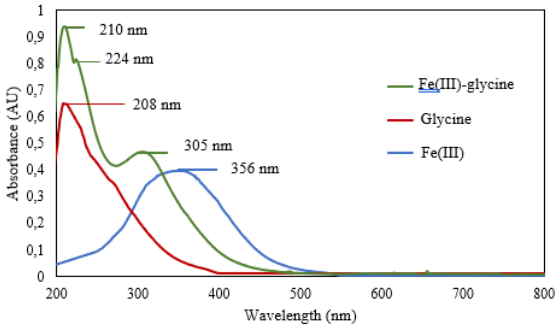

Figure 1. UV-Vis spectrum of Fe(III)-glycine complex compound

Fig. 3 displays the UV-Vis spectrum of the [$Fe(Gly)_3$] complex, which exhibits absorption peaks at 210, 224, and 305 nm. These peaks indicate the presence of electronic transitions within the complex, particularly those associated with ligand-to-metal charge transfer (LMCT) or d–d transitions. Compared to the absorption spectrum of $FeCl_3 \cdot 6H_2O$, a hypsochromic shift (shift to shorter wavelengths) is observed. This shift is likely due to the substitution of chloride ligands by glycine, as well as solvent effects that alter the electronic environment around the Fe^{3+} center, thereby lowering the energy of electronic transitions and resulting in shifts in absorption maxima [16].

The characterization of the [$Fe(Gly)_3$] complex was further carried out using infrared (IR) spectroscopy to identify the functional group interactions between the glycine ligand and the central Fe(III) metal ion, as illustrated in **Fig. 4**.

The IR spectrum shows a broad absorption band at 3408 cm^{-1}, which can be attributed to N–H stretching vibrations, while the band observed at 3014 cm^{-1} is associated with the stretching vibration of the $–NH_2$ group. The absorption band at 1637 cm^{-1} corresponds to the carbonyl (C=O) stretching vibration, and the band at 1109 cm^{-1} is assigned to C–O stretching.

In the lower wavenumber region, a band observed at 592 cm^{-1} is reasonably attributed to the Fe–O stretching vibration, supporting the coordination between the metal center and the oxygen atom of glycine. However, the assignment of the band at 898 cm^{-1} to the Fe–N stretching vibration should be treated with caution. Typically, ν(Fe–N) vibrations for amine ligands are reported at lower frequencies (generally below 600 cm^{-1}). Therefore, the band at 898 cm^{-1} is more likely associated with ligand-related vibrations, such as C–N stretching or other skeletal modes, rather than a direct Fe–N bond.

Overall, the FTIR data suggest that glycine coordinates to the Fe(III) ion, most plausibly through the oxygen atom of the carboxylate group and potentially the nitrogen atom of the amine group. However, confirmation of Fe–N coordination cannot be conclusively established based solely on the observed band at 898 cm^{-1} and requires further supporting evidence from complementary techniques. These signals indicate that both the nitrogen and oxygen atoms of glycine have coordinated to the Fe(III) ion, confirming the formation of a stable coordination complex [16]

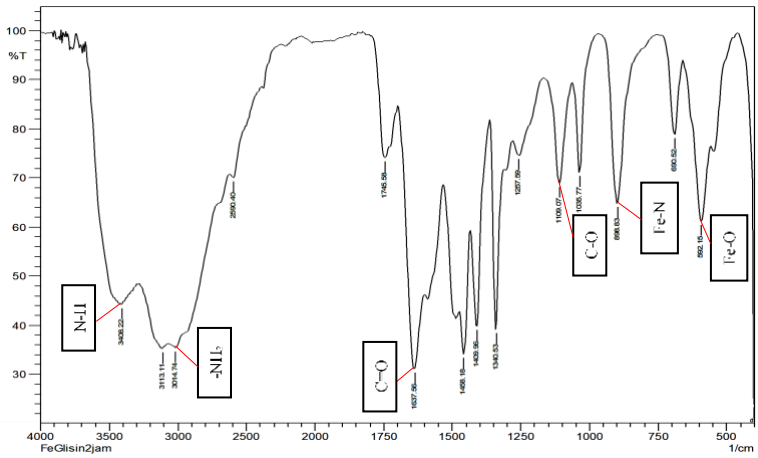

Figure 4. IR spectrum of the Fe(III)-glycine complex compound

Table 1. Absorption area of the Fe(III)-glycine complex compound

Function Group	Wavenumber (cm^{-1})	
	Fe(III)-Glycine	Reference (Kudrat *et al*, 2015)
N-H	3,408	3,413
$N-H_2$	3,014	3,047
C=O	1,637	1,574
C-O	1,109	1,107
Fe-N	898	823
Fe-O	592	523

Antidiabetic Activity Test Results. The antidiabetic activity test of the $[Fe(Gly)_3]$ complex was conducted in vivo using male mice (Mus musculus L.) with body weight and blood glucose levels as primary parameters. The study consisted of several groups: a normal control group (received only food and water), a negative control group (induced with alloxan without treatment), and a positive control group (administered glibenclamide at a dose of 5 mg/kg body weight). In the second week, diabetes was induced in the male mice by subcutaneous injection of alloxan at a dose of 150 mg/kg body weight in the dorsal neck region. After confirmation of hyperglycemia, oral treatment was administered using the $[Fe(Gly)_3]$ complex at varying doses of 50, 100, and 200 µg/kg body weight. For comparison, $FeCl_3 \cdot 6H_2O$ and pure glycine were also administered at doses of 50 and 200 µg/kg body weight. Observations were carried out over a 4-week period, during which body weight and blood glucose levels were recorded weekly to evaluate the antidiabetic efficacy of the synthesized complex.

Table 2. Elemental (CHN) Analysis of Fe(III)-Glycine Complex

Element	Theoretical (%) $[Fe(Gly)_3]$	Experimental (%)	Deviation (%)
C	30.02	29.85	−0.17
H	5.04	5.12	+0.08
N	17.52	17.30	−0.22

The elemental (CHN) analysis showed good agreement between the experimental and theoretical values for the proposed $[Fe(Gly)_3]$ complex. The small deviations (< ±0.5%) indicate that the synthesized compound has a composition consistent with the expected 1:3 metal-to-ligand stoichiometry, thereby supporting the successful formation of the Fe(III)-glycine complex (table 2).

Mice Body Weight. The doses of alloxan, glibenclamide, and the synthesized complex were determined based on the body weight of each male mouse. Body weight measurements were conducted once per week in accordance with each stage of the treatment protocol. The average body weight data of the male mice throughout the treatment period are presented in **Fig. 5**.

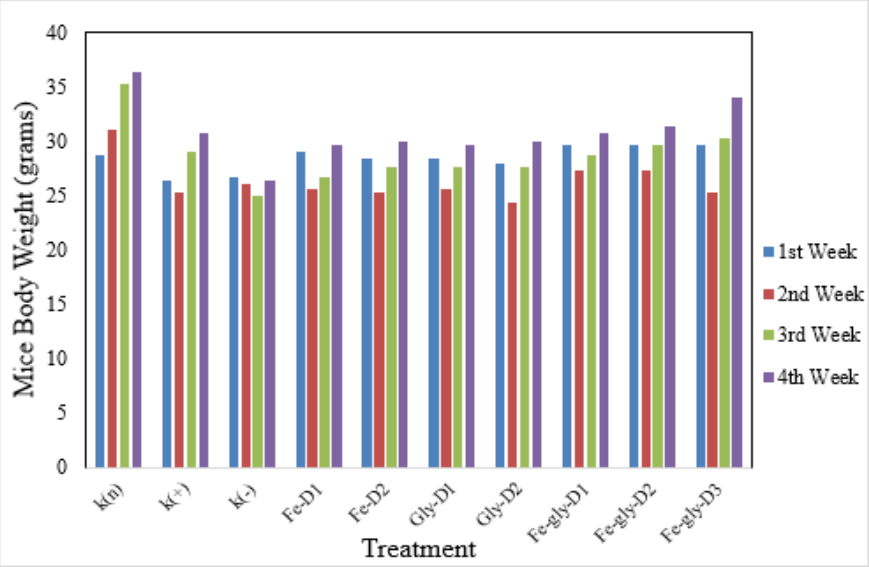

Figure 5. Average body weight of male mice

Fig. 5 displays the average body weight of male mice over a 4-week period. In the first week, the mice underwent an acclimatization phase and exhibited stable body weights ranging from 26 to 30 grams. Alloxan induction was performed in the second week, resulting in a decrease in body weight to approximately 25–28 grams. This reduction in body weight is attributed to the mechanism of action of alloxan, which structurally resembles glucose and competes with it for binding to glucose transporters (GLUT2) in pancreatic β-cells. Once internalized, alloxan induces oxidative stress and damages the β-cells, impairing the synthesis of glycogen and lipids, thereby leading to weight loss [17][18]. In contrast, mice in the normal control group did not exhibit weight loss since they were not subjected to any treatment aside from standard food and water. The positive and negative control groups, both induced with alloxan, exhibited typical diabetic symptoms such as dehydration, increased water intake (polydipsia), and frequent urination (polyuria), contributing further to the observed weight reduction.

In the third and fourth weeks, the positive control group of mice received treatment with glibenclamide, which resulted in an increase in body weight to approximately 29–31 grams. Glibenclamide is a widely used sulfonylurea-class oral antidiabetic drug indicated for type 2 diabetes mellitus. Its primary mechanism of action involves stimulating pancreatic β-cells to enhance insulin secretion. Insulin exerts anabolic effects by promoting glucose uptake and metabolism in peripheral tissues, particularly in muscle and adipose tissue. The glucose is utilized for the synthesis of glycogen, fatty acids, and proteins. These metabolic activities contribute to an increase in muscle and fat mass, thereby leading to weight gain [19].

The treatment group receiving the $[Fe(Gly)_3]$ complex exhibited a response comparable to that of the glibenclamide-treated group. The $[Fe(Gly)_3]$ complex demonstrated an anti-hyperglycemic effect in male mice induced with alloxan, as evidenced by an increase in body weight during the third and fourth weeks, reaching approximately 29–34 grams. This weight gain suggests that the $[Fe(Gly)_3]$ complex possesses glucose-lowering activity in diabetic mice. The proposed mechanism involves stimulation of insulin secretion and enhanced glucose uptake by body cells, like the action of established antidiabetic agents such as glibenclamide [20].

Blood Sugar Levels of Mice. Blood glucose levels in mice were measured four times throughout the treatment period using the synthesized $[Fe(Gly)_3]$ complex. Each treatment was replicated three times (triplicate) to ensure data reliability. The results from the treatment group were compared to those of the positive control group (K^+), as shown in **Fig. 6**.

Fig. 6 presents the blood glucose levels of male mice from all treatment groups. In the second week, mice were induced with alloxan at doses adjusted according to their body weights. Alloxan is known to cause selective destruction of pancreatic β-cells, thereby reducing insulin production and inducing type 1 diabetes mellitus [21]. Pancreatic cell damage caused by alloxan—either through oxidative stress, inflammation, or other metabolic disruptions—leads to impaired insulin secretion, which is essential for glucose regulation. Consequently, blood glucose levels rise significantly. The results of blood glucose measurements after treatment, along with the average glucose lowering percentage (%GL), are presented in **Table 3**

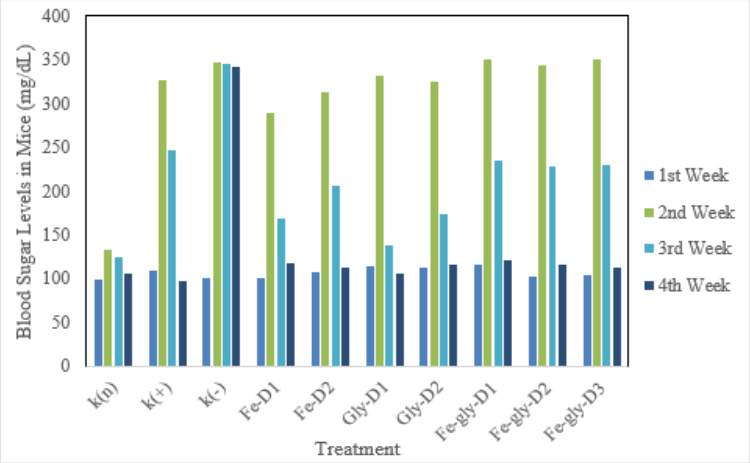

Figure 6. Blood sugar levels of male mice

Table 3. Average percentage of blood sugar levels in male mice

Treatment	Blood Sugar Levels in Mice (%)
Fe-gly-D1 (50 µg/kg BB)	65.71
Fe-gly-D2 (100 µg/kg BB)	66.47
Fe-gly-D3 (200 µg/kg BB)	68.00
Fe-D1 (50 µg/kg BB)	59.31
Fe-D2 (200 µg/kg BB)	63.90
Gly-D1 (50 µg/kg BB)	68.07
Gly-D2 (200 µg/kg BB)	64.51
K(n)	4.54
K(+)	70.20
K(-)	1.15

Table 4. Results of ANOVA and BNT 5% statistical test

Treatment	Average Blood Sugar Levels of Mice (Mean ± Std. Deviasi)
Fe-gly-D1 (50 µg/kg bb)	(120.33 ± 5.51) [a]
Fe-gly-D2 (100 µg/kg bb)	(115.33 ± 3.06) [a]
Fe-gly-D3 (200 µg/kg bb)	(112.00 ± 4.58) [a]
Fe-D1 (50 µg/kg bb)	(118.33 ± 17.67) [a]
Fe-D2 (200 µg/kg bb)	(112.67 ± 13.32) [a]
Gly-D1 (50 µg/kg bb)	(106.33 ± 7.10) [a]
Gly-D2 (200 µg/kg bb)	(115.33 ± 2.09) [a]
K(n)	(105.00 ± 6.25) [a]
K (+)	(97.00 ± 12.53) [a]
K (-)	(342.33 ± 5.13) [b]

Note: Different superscript letters (a, b) within the same column indicate statistically significant differences between groups. Values sharing the same superscript letter are not significantly different at $p < 0.05$.

Table 3 presents the average percentage of blood glucose reduction in mice after treatment with $FeCl_3$, glycine ligand, and the $[Fe(Gly)_3]$ complex. The control groups—normal, positive, and negative—showed glucose reduction percentages of 4.54%, 70.20%, and 1.15%, respectively. In the treatment group receiving Fe(III), the 50 µg/kg BW dose led to a glucose reduction of 59.31%, while the 200 µg/kg BW dose resulted in a reduction of 63.90%. Similarly, treatment with the glycine ligand produced reductions of 68.07% at 50 µg/kg BW and 64.51% at 200 µg/kg BW. For the $[Fe(Gly)_3]$ complex, which was tested at three different doses—50, 100, and 200 µg/kg BW—the corresponding glucose reduction percentages were 65.71%, 66.47%, and 68.00%. As shown in Table 2, the 200 µg/kg BW dose of the $[Fe(Gly)_3]$ complex exhibited the highest glucose-lowering activity among the tested doses, approaching the effectiveness of the positive control group (70.20%). These results suggest that the $[Fe(Gly)_3]$ complex has promising antidiabetic potential comparable to standard drugs like glibenclamide.

ANOVA test. Values are expressed as mean ± standard deviation (SD). Statistical analysis was performed using one-way Analysis of Variance (ANOVA), followed by the Least Significant Difference (LSD) post-hoc test at the 5% significance level ($p < 0.05$) (previously referred to as BNT 5%). The results of the ANOVA test for all treatment groups are presented in **Table 4**.

As shown in **Tables 3 and 4**, the mean blood glucose levels and the mean ± SD values of the $[Fe(Gly)_3]$ treatment groups (doses 1, 2, and 3) were compared to the positive control (K^+), which had a mean ± SD of 97.00 ± 12.53. The $[Fe(Gly)_3]$ dose 3 group (200 µg/kg BW) showed a mean ± SD of 112.00 ± 4.58, which is the closest to the positive control. Moreover, Table 2 shows that the $[Fe(Gly)_3]$ D3 group (200 µg/kg BW) achieved a glucose-lowering percentage of 68%, which is close to the positive control group's 70.20%. These findings indicate that the 200 µg/kg BW dose of the Fe(III)-glycine complex is the most effective in reducing blood glucose levels in alloxan-induced diabetic mice.

As shown in **Table 4**, a statistically significant difference was observed between the negative diabetic control group and all other treatment groups, indicating that the administered treatments were effective in reducing blood glucose levels compared to untreated diabetic mice.

Interestingly, no significant differences were observed between the normal control group and the positive control group, as well as several treatment groups, including those receiving [$Fe(Gly)_3$], $FeCl_3$, and glycine at specific doses. This observation may suggest that these treatments were able to reduce blood glucose levels toward near-normal values.

However, this result should be interpreted with caution. The absence of significant differences between the normal and treated groups may be influenced by factors such as limited sample size, variability within groups, or the degree of diabetes induction achieved by alloxan. Incomplete or variable β-cell destruction in the alloxan-induced model may result in partial recovery of glycemic control, thereby reducing detectable differences between groups.

Therefore, while the findings indicate a potential glucose-lowering effect of the Fe(III)-glycine complex and its components, further studies with larger sample sizes, stricter model validation, and additional biomarkers are necessary to confirm the robustness and reproducibility of these results. Vital Organ Test of Mice. Male mice affected by diabetes tend to experience damage to vital organs due to persistent hyperglycemia. Chronic hyperglycemia induces excessive oxidative stress, leading to the generation of free radicals that compromise cell membranes and damage tissues. As a result, several vital organs in diabetic male mice may be impaired, including:

Liver. The first vital organ affected in diabetic male mice is the liver. This is due to the liver's central role in glucose metabolism, including gluconeogenesis, glycogenolysis, and glycogen storage. During hyperglycemia, the liver is forced to work harder to reduce and stabilize blood glucose levels. Prolonged exposure to such metabolic stress can lead to both structural and functional damage to the liver (**Fig. 7**).

Fig. 7 illustrates swelling of the liver in mice. Excessive glucose intake leads the liver to increase fatty acid synthesis, which subsequently accumulates in hepatic tissue. This lipid accumulation can trigger inflammation (hepatitis) and, over time, may progress to liver cirrhosis, permanent scarring of liver tissue. As a result, the liver undergoes enlargement or hypertrophy (hepatomegaly) in diabetic mice with prolonged hyperglycemia [22].

Pancreas. The pancreas plays a vital role in producing insulin, the primary hormone responsible for regulating blood glucose levels. When abnormalities or damage occur in the pancreatic β (beta) cells, insulin production may significantly decrease or cease entirely. This disruption leads to uncontrolled blood glucose levels and the onset of diabetes mellitus. **Fig. 8** illustrates the impaired pancreatic function associated with this condition.

Fig. 8 shows that the pancreas of diabetic male mice exhibits an increase in size. This enlargement is attributed to the proliferation of pancreatic cells as a compensatory response to persistently elevated blood glucose levels (hyperglycemia) [23].

Kidney. The kidneys contain numerous small blood vessels (glomeruli) that are highly susceptible to damage from elevated blood glucose levels in diabetic conditions. Persistent hyperglycemia can impair the structure of renal blood vessels, disrupt the filtration process, and reduce the kidneys' ability to eliminate waste products from the bloodstream. **Fig. 9** illustrates kidney damage associated with this condition.

Diabetes is often associated with high blood pressure (hypertension), which is a major risk factor for kidney damage. Hypertension can exacerbate injury to renal blood vessels, leading to renal fibrosis and an increased number of renal tubules exhibiting lesions (damage or injury). In addition, diabetic neuropathy can impair the function of smooth muscle in the kidneys, further reducing their filtration capacity [24].

Heart. The heart of diabetic mice exhibits morphological changes, including an increase in size (cardiomegaly). This condition is caused by cardiac muscle hypertrophy as a compensatory response to the increased workload due to metabolic disturbances. In addition, thinning of the heart walls is observed, as the cardiomyocytes become more fragile and attenuated due to cellular damage induced by oxidative stress and chronic hyperglycemia (**Fig. 10**).

Fig. 10 shows swelling of the heart in diabetic mice. Elevated blood glucose levels increase the risk of atherosclerotic plaque formation along arterial walls. This occurs because chronic hyperglycemia damages endothelial cells and triggers inflammatory responses. The resulting atherosclerotic plaques can narrow or harden the arteries, restricting blood flow to the heart and potentially leading to myocardial damage [25].

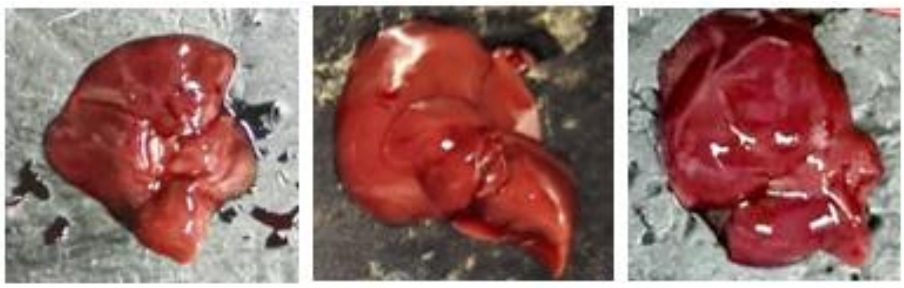

Figure 2. Male mouse organs (a) normal control, (b) negative control, (c) Fe(III)-Glycine

Figure 8. Pancreatic organs of mice (a) normal control, (b) negative control, (c) Fe(III)-Glycine

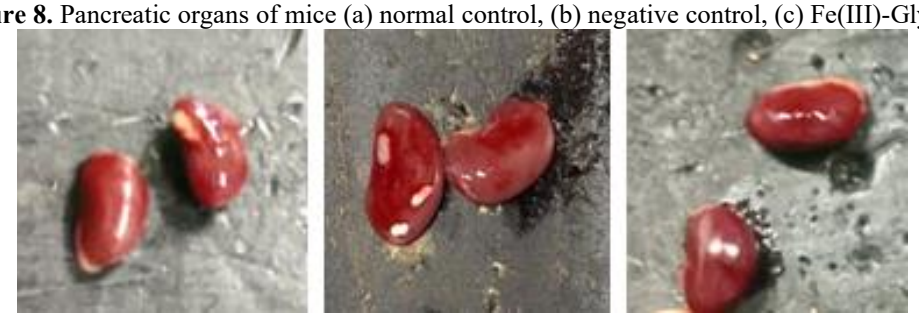

Figure 9. Kidney organs of mice (a) normal control, (b) negative control, (c) Fe(III)-Glycine

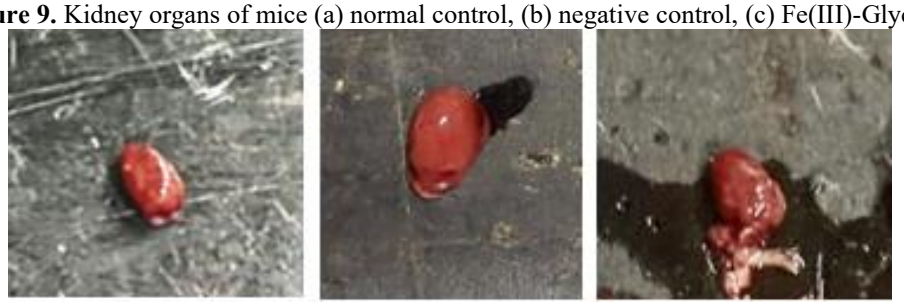

Figure 10. Heart organs of mice (a) normal control, (b) negative control, (c) Fe(III)-Glycine

Based on the evaluation of several vital organs, it can be concluded that diabetes induces functional impairments in the vital organs of male mice. Swelling was observed in the liver, pancreas, and heart, along with darkened coloration of the kidneys, indicating tissue damage and organ dysfunction.

Pharmacokinetic Results of Fe(III)-Glycine Complex Compounds. Pharmacokinetic profiling was conducted using the Lipinski's Rule of Five and Protox-II websites. The purpose of this analysis is to assess the drug-likeness and potential of the synthesized compound as a candidate for antidiabetic therapy. In this study, the $[Fe(Gly)_3]$ complex was evaluated and compared with glibenclamide as a reference compound. Glibenclamide was selected as a comparator because it is a widely used antidiabetic drug in the treatment of type 2 diabetes mellitus.

Drug-likeness analysis is commonly evaluated using Lipinski's Rule of Five, which provides general criteria for the oral bioavailability of small organic molecules, including molecular weight (< 500 Da), log P (< 5), hydrogen bond donors (< 5), and hydrogen bond acceptors (< 10) [25]. However, it is important to note that these rules were originally developed for purely organic compounds and may not be directly applicable to metal-based complexes.

In the case of the $[Fe(Gly)_3]$ complex, the application of Lipinski's parameters should be

interpreted with caution. Metal complexes may undergo partial or complete dissociation under physiological conditions, particularly in the acidic environment of the gastrointestinal tract. As a result, calculated properties such as log P and molecular descriptors for the intact complex may not accurately reflect its actual behavior in vivo.

Therefore, the Lipinski-based analysis presented in **Table 5** should be considered as a preliminary physicochemical assessment rather than a definitive predictor of oral bioavailability. Similarly, the ADMET and toxicity predictions for the intact complex may not fully represent its biological fate, as the active species in vivo could differ from the original coordination complex.

Despite these limitations, the computational results may still provide useful initial insights into the potential pharmacokinetic behavior and safety profile of the system. Nevertheless, further experimental studies, including stability, speciation, and metabolic investigations, are required to better understand the behavior of the Fe(III)-glycine complex under physiological conditions.The pharmacokinetic analysis results based on Lipinski's Rule of Five are presented in **Table 5**.

Table 5. Lipinski Rule of Five Analysis Results

Compound Name	BM	H Bond Donor	H-Bond Acceptor	Log P	Molar Refraction	Eligible/Not Eligible
Standar	<500	<5	<10	<5	40-130	Eligible
Glibenclamide	498	3	8	3.9	123	Eligible
[Fe(Gly)3]	238	3	9	-5,92	40,63	Eligible

Table 6. Protox-II Prediction Results

	Target	Shorthand	Computational Prediction	Possibility (%)
Glibenclamide	Hepatoxicity	Dili	Inactive	0.63
	Carcinogenicity	Carcinoma	Inactive	0.76
	Immunotoxicity	Immuno	Inactive	0.73
	Mutagenicity	Mutagen	Inactive	0.80
	Cytotoxicity	Sito	Inactive	0.77
$[Fe(Gly)_3]$	Hepatoxicity	Dili	Inactive	0.72
	Carcinogenicity	Carcinoma	Inactive	0.52
	Immunotoxicity	Immuno	Inactive	0.99
	Mutagenicity	Mutagen	Inactive	0.52
	Cytotoxicity	Sito	Inactive	0.58

Data in **Table 5** show that glibenclamide has a molecular weight of 498 g/mol, three hydrogen bond donors, eight hydrogen bond acceptors, a log P value of 3.9, and a molar refractivity of 123. In comparison, the $[Fe(Gly)_3]$ complex has a molecular weight of 238 g/mol, three hydrogen bond donors, nine hydrogen bond acceptors, a log P value of -5.92, and a molar refractivity of 40.63. Based on these parameters, both glibenclamide and the $[Fe(Gly)_3]$ complex satisfy the Lipinski's Rule of Five, indicating their potential as orally active drug candidates.

The next pharmacokinetic assessment was conducted using the Protox-II platform. The Protox-II server provides predictive information on various toxicity parameters, including acute oral toxicity in mice (LD_{50}), toxicity class, as well as potential hepatotoxicity, carcinogenicity, immunotoxicity, mutagenicity, and cytotoxicity. The predicted pharmacokinetic and toxicity profiles of glibenclamide and the $[Fe(Gly)_3]$ complex, as analyzed by Protox-II, are presented in **Table 6**.

Table 6 presents the pharmacokinetic results from the Protox-II analysis, showing that both glibenclamide and the $[Fe(Gly)_3]$ complex were classified as "inactive" for all tested toxicity parameters, including hepatotoxicity, carcinogenicity, immunotoxicity, mutagenicity, and cytotoxicity. These findings suggest that glibenclamide and the $[Fe(Gly)_3]$ complex have the potential to be developed as drug candidates, as they meet the safety criteria established by the Protox-II server and exhibit no significant predicted toxicity.

The antidiabetic activity observed for the Fe(III)-glycine complex cannot be primarily attributed to the stimulation of insulin secretion, as the experimental model employed in this study involves alloxan-induced diabetes, which is characterized by the selective destruction of pancreatic β-cells. Under such conditions,

endogenous insulin production is significantly impaired, making insulin secretagogue mechanisms less plausible.

Instead, the observed hypoglycemic effect of the Fe(III)-glycine complex may be associated with alternative pathways. One possible mechanism is the enhancement of glucose uptake in peripheral tissues, thereby improving glucose utilization independent of insulin secretion. In addition, the complex may contribute to improved insulin sensitivity in residual functional tissues, which could partially compensate for insulin deficiency.

Another plausible mechanism involves the antioxidant properties of Fe(III). As discussed in the introduction, iron plays a role in enzymatic systems that regulate oxidative stress. The Fe(III)-glycine complex may help reduce oxidative stress by modulating reactive oxygen species (ROS), which are known to contribute to β-cell damage and the progression of diabetes. By mitigating oxidative stress, the complex could protect remaining pancreatic tissue and improve overall metabolic homeostasis.

Furthermore, glycine as a ligand may enhance the bioavailability and biocompatibility of the complex, potentially facilitating its interaction with biological systems and improving its pharmacological effect.

Overall, the antidiabetic activity of the Fe(III)-glycine complex is more likely mediated through a combination of antioxidant effects and improved peripheral glucose utilization rather than direct stimulation of insulin secretion. However, further studies at the molecular level are required to elucidate the precise mechanism of action.

4 Conclusion

The $[Fe(Gly)_3]$ complex was successfully synthesized under optimal conditions at a reaction time of 2 hours and pH 7. Characterization results showed distinctive UV-Vis absorption peaks at 210, 224, and 305 nm, while IR spectra revealed absorption bands at 592 cm^{-1} for Fe–O and 898 cm^{-1} for Fe–N bonds. The antidiabetic activity test demonstrated that a dose of 200 µg/kg body weight effectively reduced blood glucose levels in mice by 68%. Statistical analysis using ANOVA indicated no significant differences among the treatment group means, and further analysis using the 5% LSD test revealed that the negative control group differed significantly, whereas the $[Fe(Gly)_3]$ complex, Fe(III) ion, glycine ligand, and both the positive and normal control groups showed no significant differences. Based on pharmacokinetic evaluation, the $[Fe(Gly)_3]$ complex meets the criteria for drug-likeness and has potential as a candidate for antidiabetic drug development.

Acknowledgement

This research was supported by the Integrated Laboratory and Center for Technological Innovation, as well as the Department of Chemistry, University of Lampung.

References

[1] Magliano, D. J., & Boyko, E. J. (2021). IDF diabetes atlas (10th ed.). International Diabetes Federation.

[2] Ministry of Health Republic of Indonesia. (2020). Stay productive, prevent, and manage diabetes mellitus. Data and Information Center.

[3] Maharani, A., & Ghinan, M. (2024). Literature review: Risk factors for type II diabetes mellitus in adolescents. Jurnal Sehat Mandiri, 19(1). https://doi.org/10.33761/jsm.v19i1.1395

[4] Sakurai, H., Katoh, A., Kiss, T., Jakusch, T., & Hattori, M. (2010). Metallo-allixinate complexes with antidiabetic and anti-metabolic syndrome activities. Metallomics, 2(10), 670–682. https://doi.org/10.1039/c0mt00025f

[5] Ambarwati, Y., Rizky, Y., Bahri, S., & Laila, A. (2021). Synthesis and antidiabetic bioactivity test of Cr(III)-glycine complex in male mice (Mus musculus L.). In Proceedings of the 3rd International Conference on Applied Sciences, Mathematics, and Informatics (ICASMI).

[6] Ambarwati, Y., Yunianti, R., Bahri, S., & Laila, A. (2022). Synthesis and antidiabetic test of Cu(II)-glycine complex compounds. In Proceedings of the 4th International Conference on Applied Sciences, Mathematics, and Informatics (ICASMI). https://doi.org/10.1063/5.0208474

[7] Ambarwati, Y., Martoprawiro, M. A., Mulyani, I., Ismunandar, & Onggo, D. (2019). Docking interaction of chromium(III) phenylalanine with protein tyrosine phosphatase. Journal of Physics: Conference Series, 1338(1), 012009. https://doi.org/10.1088/1742-6596/1338/1/012009

[8] Ambarwati, Y., Septiani, L., Bahri, S., Yandri, Hadi, S., & Kesumaningrum, N. D. (2020). Antidiabetic bioactivity test of Cr(III) and Cu(II) complex compounds on mice (Mus musculus L.). IOP Conference Series: Earth and Environmental Science, 537(1), 012045. https://doi.org/10.1088/1755-1315/537/1/012045

[9] Ambarwati, Y., Firguna, D. S., Bahri, S., Laila, A., & Hadi, S. (2021). Synthesis of Cr(III) aspartate and Cu(II) aspartate complexes as antidiabetic compounds. Indonesian Journal of Pharmacy, 32(4), 539–547. https://doi.org/10.22146/ijp.2484

[10] Kongot, M., Reddy, D. S., Singh, V., Patel, R., Singhal, N. K., & Kumar, A. (2019). Oxidovanadium (IV) and iron (III) complexes as plausible antidiabetic candidates. Applied Organometallic Chemistry, 34(2), e5327. https://doi.org/10.1002/aoc.5327

[11] Knapp, M. J. (2014). Preface: Gas and redox sensors special issue. Journal of Inorganic Biochemistry, 133, 57. https://doi.org/10.1016/j.jinorgbio.2014.02.008

[12] Liang, J., Huang, Y. B., & Cao, R. (2019). Metal–organic frameworks for CO_2 fixation. Coordination Chemistry Reviews, 378, 32–65. https://doi.org/10.1016/j.ccr.2017.11.013

[13] Konapalli, N. R., Sakamuri, A., Rao, K. R., Reddy, R., Kumar, P., Satyanarayana, S., & Manchala, R. (2015). Effect of chromium(III) amino acid complexes on insulin resistance. Journal of Diabetes and Obesity, 2(1). https://doi.org/10.15436/2376-0494.15.016

[14] Brown, J. A., Chaparro, A. L., McCarthy, L. C., Moniodes, S. C., Ostrowski, E. E., & Carroll, M. E. (2021). Iron tricarbonyl α-diimine complexes. Polyhedron, 203, 115168. https://doi.org/10.1016/j.poly.2021.115168

[15] Stuart, B. H. (2004). Infrared spectroscopy: Fundamentals and applications. John Wiley & Sons. https://doi.org/10.1002/0470011149

[16] Guan, J., Fan, L., Liu, Y. N., Shi, B., Yuan, J., Zhang, R., et al. (2020). Fe(III) complex in polyamide membranes. Journal of Membrane Science, 602, 117980. https://doi.org/10.1016/j.memsci.2020.117980

[17] Haryanto, H., Sutandi, A., Kusumawati, E., Nurhayati, S., Fitri, F. M., Nafsi, G., & Nuraeni, S. W. (2023). Curculigo latifolia extracts in alloxan-induced diabetes. Biosaintifika, 15(3), 370–377. https://doi.org/10.15294/biosaintifika.v15i3.40498

[18] Zhang, H. J., Chen, C., Ding, L., Shi, H. H., Wang, C. C., Xue, C. H., et al. (2020). Sterol sulfate alleviates insulin resistance. Pharmacological Research, 160, 105191. https://doi.org/10.1016/j.phrs.2020.105191

[19] Kamalakkannan, N., & Prince, P. S. (2006). Antihyperglycaemic effect of rutin. Basic & Clinical Pharmacology & Toxicology, 98(1), 97–103. https://doi.org/10.1111/j.1742-7843.2006.pto_241.x

[20] Norton, L., Shannon, C., Gastaldelli, A., & DeFronzo, R. A. (2022). Insulin as the master regulator of glucose metabolism. Metabolism, 129, 155142. https://doi.org/10.1016/j.metabol.2022.155142

[21] DeFronzo, R. A. (2004). Pathogenesis of type 2 diabetes mellitus. Medical Clinics of North America, 88(4), 787–835. https://doi.org/10.1016/j.mcna.2004.04.013

[22] Lim, S., Tie, H. H., Law, C. L., & Ghulam, R. R. (2012). Antidiabetic properties of red yeast rice extract. Experimental and Clinical Endocrinology & Diabetes, 120(10).

[23] Singh, S. P., & Yadava, D. K. (2011). Protective effect of Tinospora cordifolia. Journal of Ethnopharmacology, 137(1).

[24] Li, H., Cao, C., & Wu, Y. (2018). Amino acid complexes of zinc as antidiabetic agents. Bioorganic Chemistry, 78.

[25] Berthias, F., Wang, Y., Alhajji, E., Rieul, B., Moussa, F., Benoist, J. F., & Maitre, P. (2020). Identification of amino acids using spectrometry. Analytical Methods, 12(14). https://doi.org/10.1039/d0an00377h

[26] Rabie, M. (2022). Natural inhibitors of coronavirus main protease. International Journal of New Chemistry, 9(3), 225–237. https://doi.org/10.22034/ijnc.2022.3.10